Modeling and Hardware-in-the-Loop System Realization of Electric Machine Drives – A Review

Jae Suk Lee, *Member, IEEE*, and Gilsu Choi, *Member, IEEE*

***Abstract*— This paper presents a state-of-the-art review in modeling approach of hardware in the loop simulation (HILS) realization of electric machine drives using commercial real time machines. HILS implementation using digital signal processors (DSPs) and field programmable gate array (FPGA) for electric machine drives has been investigated but those methods have drawbacks such as complexity in development and verification. Among various HILS implementation approaches, more efficient development and verification for electric machine drives can be achieved through use of commercial real time machines. As well as implementation of the HILS, accurate modeling of a control target system plays an important role. Therefore, modeling trend in electric machine drives for HILS implementation is needed to be reviewed. This paper provides a background of HILS and commercially available real time machines and characteristics of each real time machine are introduced. Also, recent trends and progress of permanent magnet synchronous machines (PMSMs) modeling are presented for providing more accurate HILS implementation approaches in this paper**.

***Index Terms*— Hardware-in-the-loop, machine modeling, permanent magnet synchronous machine (PMSM), model based design.**

NOMENCLATURE

v_d, v_q	d & q axis voltages [V]
i_d, i_q	d & q axis stator currents [A]
i_a, i_b, i_c	a, b, and c phase currents [A]
L_d, L_q	d & q axis inductances [H]
λ_d, λ_q	d & q axis flux linkages [Weber]
R_s	stator resistance [Ω]
T_e	electromagnetic torque [Nm]
P	number of poles
λ_{pm}	magnet flux linkage [Weber]
ω_e	synchronous speed [Rad/s]
θ	rotor angle [Rad]
W	stored energy [J]
L_{dd}^{dyn}, L_{qq}^{dyn}	dynamic d & q axis self inductance [H]
L_{dq}^{dyn}, L_{qd}^{dyn}	dynamic d & q axis mutual inductance [H]
μ	ratio of faulted turns to total number of turns
v_f, i_f	fault voltage [V], current [A]
R_f	fault resistance [Ω]
λ_f	flux linkage in faulted turns [Weber]

Manuscript received October 20, 2020; revised May 05, 2021; accepted August 03, 2021. date of publication September 25, 2021; date of current version September 18, 2021.

This work was supported in part by the National Research Foundation of Korea (NRF) grant funded by Korea government (No.2020R1C1C1013260) and in part by INHA UNIVERSITY Research Grant. (*Corresponding author: Gilsu Choi*)

J. Lee is with the Jeonbuk National University, Jeonju, Jeonbuk, Korea (e-mail: jaesuk@ jbnu.ac.kr).

G. Choi is with Inha University, Incheon, Korea (e-mail: gchoi@ inha.ac.kr).

Digital Object Identifier 10.30941/CESTEMS.2021.00023

I. INTRODUCTION

THE, use of electrified transportation systems, including electric vehicles (EVs) and more electric aircraft (MEA), has increased as technologies for electric motor drives and power electronics have improved. Electric traction drive systems are a core component of electrified transportation systems, and development and analysis of such systems is critical. Similar to semiconductors and signal processor technology, real-time simulation techniques have become more available for the development and analysis of the potential industrial applications of such systems. [1-3].

A real-time simulation that involves a target system in a loop is typically referred to as a Hardware-in-the-Loop simulation (HILS). Such systems allow for real-time simulation of an entire control target, as well as gradual integration with a developed target system. As a result, development time and costs are significantly reduced. The benefits of real-time simulation have resulted in its widespread use in the development of new applications that rely on electric motor drives, which include power converters, electric machines, and associated control algorithms [4-6]. Real-time simulation of an electric motor drive involves real-time control and the development of an electric machine model. Real-time control necessitates that programming either be manually generated or directly generated from a simulation model through a code translator. When manual programming is performed, microcontrollers, field programmable gate arrays (FPGA), and digital signal processors (DSP) are generally used. A DSP is a widely-used processor, relied upon for its high performance and multi-functional features. A FPGA is a cost-effective device with strong computational capabilities that have been extensively analyzed [7]-[9], particularly for its HILS applications [10], [11]. Electric motor drive systems are often complex, and calculation and signal processing time are therefore often barriers to the implementation of real-time control. To overcome this challenge, the logic design and performance of FPGAs and DSPs have been refined. Despite the attractiveness of DSPs and a FPGAs, both do still need to be programmed manually (with a different computer language for each), which can be a bottleneck on the development process and requires a high level of competence from a given

programmer.

One alternative real-time control approach using DSPs and FPGAs is to use commercially available real-time machines, including products available from Plexim and dSPACE. Signal processors or FPGAs are used in real-time machines but the difference is that the commercial real-time machines are compatible with commercial simulation software. A simulation model that includes a controller and a system model can automatically generate code, and that code can be downloaded into real-time machines. This feature reduces development and verification time and avoids programming level dependency. Though a real-time machine system cannot economically compete with a customized control board that uses a DSP or FPRA, it is well-suited to situation where an application requires rapid development and verification.

For a HILS used to develop electric motor drives, the accuracy of electric machine models is critical, as a simulation that uses an unrealistic and inaccurate model delivers only meaningless results. In this paper, we review recent trends and developments in AC machine modeling by HILS. We focus in particular on permanent magnet synchronous machine (PMSM) modeling, as PMSMs have broad industrial and automotive applications due to their high efficiency and power density. In the following sections, a model-based design process which is necessary for real-time simulation is reviewed. We also introduce commercially available real-time machines and their features. Finally, we examine recent trends in modeling methods of PMSMs for HILS implementation.

II. Model Based Design

A flow of model based design can be represented via a v-chart as shown in Fig.1.

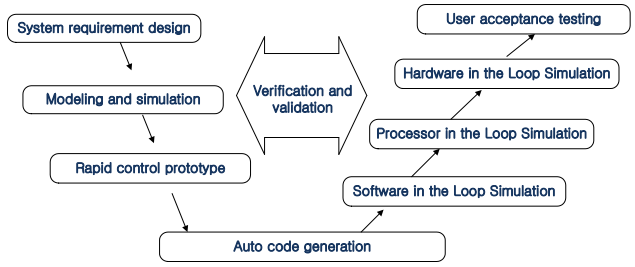

Fig. 1. A model based design process representing via a v-chart.

Fig.1 illustrates how the first and second stages of any MBD process are the development of system requirements and simulation modeling. Development of a rapid control prototype (RCP) occurs as a verification of a developed simulation model. At the RCP stage, the simulated model is connected to a real-time machine and the simulation model and the control algorithm are checked and verified to minimize potential errors. The next stage of RCP development is automatic code generation. In this stage, a computer program written in either C++ or HDL is generated and compiled automatically. Next, a software-in-the-loop-simulation (SILS) process is performed, in which the automatically generated computer programming code is downloaded to a real-time machine and verified. In the subsequent processor-in-the-loop (PIL) stage, the generated code is downloaded to the processor (DSP, MCU, FPGA, etc.), and its functionality is tested. If the software passes the test, the next stage is a hardware-in-the-loop simulation (HILS), in which a virtual control target system (a 'plant') is developed in the real-time machine. The real-time machine is connected to a processor to which the generated programming code has been downloaded. Once the entire control system for a target plant has been verified virtually through the HILS, the control processor may be directly connected to an actual target plant. If the processor is not verified through HILS, hardware or the circuit may be damaged by software errors, over-current, or over-voltage. Were such errors to be missed, the final designed product would be inherently less safe. This is particularly the case where the design has transportation applications, where safety concerns are paramount and the costs of hardware are relatively high.

At the HILS stage, the accuracy of models of the control target systems is critical. If a control target system is modeled accurately enough, actual experimental set-ups and verification processescan be replaced by HILS, reducing the costs and time of system development. Some software even provides allows the user to test a developed system against international functional safety standards, such as ISO 26262 for vehicles, DO-178B for aircraft, and EU 50128 for railway communication, signaling and processing systems, compounding the time savings.

III. Review of Real Time Machines

MBD requires the use of a real-time machine, though it may be used as either a real-time controller or as a virtual control target system (Fig. 2).

When a real-time machine is used as a virtual system (Fig. 2(a)), it is connected to an actual processor or controller so that the performance of the controller and its associated algorithm can be verified. Due to the advantage, HILS has been widely used to develop high-cost applications, such as aircraft or vehicle traction systems [1-3]. Such systems are also used where the possibilities for experimental implementation are limited, such as where there are line-to-line or line-to-ground fault conditions on the electric utility grid systems.

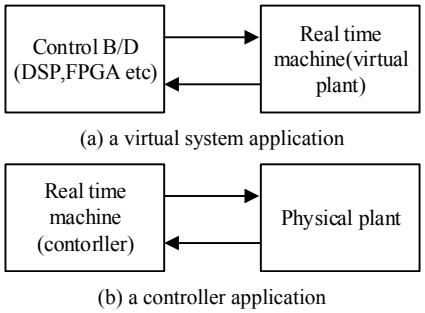

Fig. 2. Use of a real time machine by application purpose (a) a virtual system application (b) a controller application

Alternatively, a real-time machine can be used as a controller that is connected to an actual physical system (Fig. 2(b)). This approach is particularly useful to designers that are unfamiliar with signal processor hardware such as DSPs or FPGAs or computer programming languages. A real-time machine as a controller combined with an automatic code generation

function allows for rapid system development and verification. Fig. 3 shows an example of HILS environment for PMSM drives.

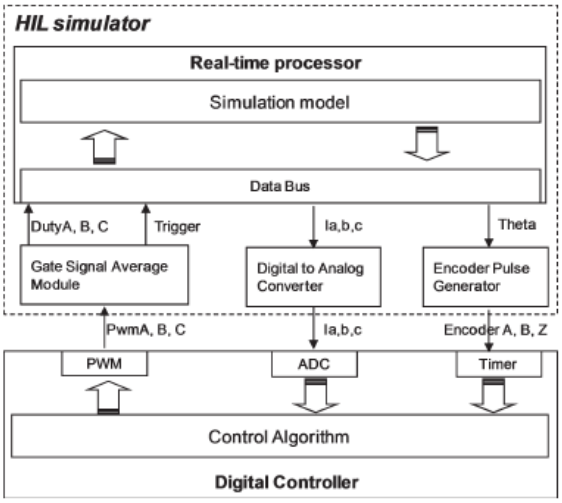

Fig.3. An example of HILS environment for PMSM drives [12]

Real-time machines are sold by a number of different commercial manufacturers. Speedgoat products (Fig. 4) are relatively more compatible with Matlab/Simulink software and their associated auto-code generation function than the machines of competitors. As seen from Fig. 4, Speedgoat products are divided by application, CPU performance, memory size, and number of analog and digital signal channels. Matlab's verification and validation toolbox can be used to verify whether the developed system meets international safety standards.

(a) Performance real time target machine(b) Education real time target machine

Fig. 4. Speedgoat real time machines [13].

dSPACE real-time machines (Fig. 5) are also compatible with Matlab/Simulink software and more dSPACE real-time machine products can be found [14].

(a) MicroLab Box (b) DS1104 R&D board

Fig. 5. dSPACE real time machines [14]

The RT-box (Fig. 6) is a real-time machine manufactured by Plexim that is used in conjunction with Plecs simulation software. Code is automatically generated through a toolbox provided by Plexim.

A real-time machine (Fig. 7) made by National Instrument (NI) is compatible with widely-used Labview software. This system's compatibility with Labview, as well as its analog and digital signal channel expandability, are its primary advantages

(a) RT box (b) RT box interface board

Fig. 6. Plexim real time machines [15]

(a) Labview (b) NI Compact Rio

Fig. 7. NI software and a real time machine [16]

over competitor real-time machines.

The TyphoonHIL-produced real-time machine (Fig. 8) is compatible with Schematic Editor and HIL Scada, software programs provided from TyphoonHIL.

Fig. 8. TyphoonHIL real time machines [17]

There are other real-time machines, including the OPAL-RT, Imperix Boombox (Fig. 9) and real-time digital simulator (RTDS), which is specified for power system analysis [18]. As each real-time machine available on the market has its own unique characteristics, users must consider performance, software compatibility, use applications, and cost when selecting a real-time machine.

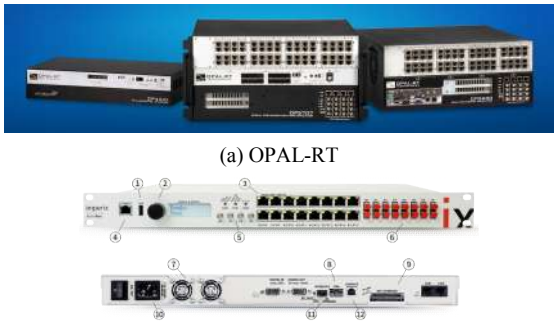

(a) OPAL-RT

(b) Imperix Boom box

Fig. 9. Plexim real time machines [19, 20]

IV. Recent Trends and Progress in AC Machine Modeling for HIL Simulation

A. Introduction

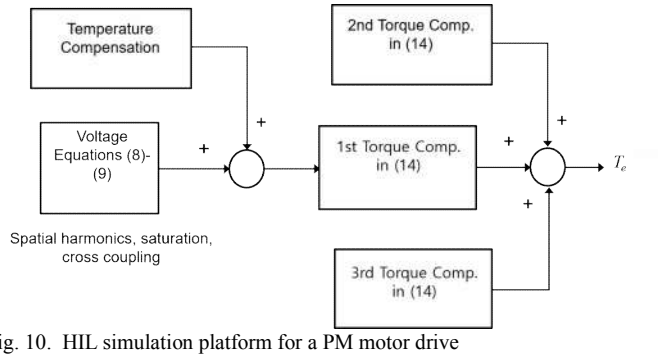

Fig. 10. HIL simulation platform for a PM motor drive

This section reviews developments in the modeling of AC electric machines, particularly PMSMs, using real-time HIL simulations. Fig. 10 shows a typical HIL simulation platform for a PM motor drive system that consists of a host computer, real-time simulator, interface board, and various physical devices. As shown in the figure, the real-time simulator includes a motor drive model that is intended to achieve a high-fidelity emulation of an actual AC motor drive system.

Growth in the HIL market over the last decade has stimulated interest in improving the modeling accuracy of electric machines in HIL simulations. Various modeling approaches and parameter identification techniques have been identified by researchers for use with several different types of electric machines. Among these modeling methods, the offline lookup table (LUT) based method used in conjunction with modified *dq* equations that take account for the impacts of saturation, cross-coupling, and spatial harmonics have so far proven to be the most promising for meeting the required accuracy thresholds in parameter estimation without a loss of computational efficiency and generality.

TABLE I summarizes AC machine characteristics that have been previously modeled for simulation by researchers. Once properly modeled, each of these characteristics can improve the modeling accuracy of HIL simulations of AC motor drive systems.

TABLE I:
AC MACHINE CHARACTERISTICS AND REFERENCES

Machine Characteristics		*References*
Machine equations		[21]-[23]
Spatial harmonics, saturation, cross coupling		[24]-[28]
Analytical modeling	MEC	[29]
	PN	[30]
	LFE	[31]
Parameter identification	Exp.	[32]-[47]
	FE/Analytic	[48]-[54]
Losses		[55]
Temperature effect		[57]
Fault conditions		[56]-[62]

B. Machine Equations

The PMSM equations for voltage, stator flux linkage, and torque in the synchronous reference frame are well-known:

$$v_d = R_s i_d + \frac{d\lambda_d}{dt} - \omega_e \lambda_q \tag{1}$$

$$v_q = R_s i_q + \frac{d\lambda_q}{dt} - \omega_e \lambda_d \tag{2}$$

$$\lambda_d = L_d i_d + \lambda_{pm} \tag{3}$$

$$\lambda_q = L_q i_q \tag{4}$$

$$T_e = \frac{3p}{4}\left(\lambda_d i_q - \lambda_q i_d\right) = \frac{3p}{4}\left(\lambda_{pm} i_q + \left(L_d - L_q\right) i_d i_q\right) \tag{5}$$

The *dq* model of a wound-field synchronous machine (WFSM) can be derived from a PMSM model in which rotor magnets are replaced with field windings and damper windings. Relevant induction machine (IM) equations have been presented by previous researchers [21-23].

To accurately predict current ripple and corresponding torque ripple, the conventional *dq* equations must be modified to account for cross-coupling and spatial harmonics [24-27]. The modified *dq* equations in the time domain are a function of *dq* stator currents and rotor position [26-28]:

$$v_d(t) = R_s i_d(t) + \frac{d\lambda_d\left(i_d, i_q, \theta\right)}{dt} - \omega_e \lambda_q\left(i_d, i_q, \theta\right) \tag{6}$$

$$v_q(t) = R_s i_q(t) + \frac{d\lambda_q\left(i_d, i_q, \theta\right)}{dt} - \omega_e \lambda_d\left(i_d, i_q, \theta\right) \tag{7}$$

By applying total differential theorem:

$$\begin{aligned} v_d(t) = {} & R_s i_d(t) + \frac{\partial \lambda_d\left(i_d, i_q, \theta\right)}{\partial i_d}\frac{di_d}{dt} - \frac{\partial \lambda_d\left(i_d, i_q, \theta\right)}{\partial i_q}\frac{di_q}{dt} \\ & + \frac{\partial \lambda_d\left(i_d, i_q, \theta\right)}{\partial \theta}\frac{d\theta}{dt} - \omega_e \lambda_q\left(i_d, i_q, \theta\right) \end{aligned} \tag{8}$$

$$\begin{aligned} v_q(t) = {} & R_s i_q(t) + \frac{\partial \lambda_q\left(i_d, i_q, \theta\right)}{\partial i_d}\frac{di_d}{dt} - \frac{\partial \lambda_q\left(i_d, i_q, \theta\right)}{\partial i_q}\frac{di_q}{dt} \\ & + \frac{\partial \lambda_q\left(i_d, i_q, \theta\right)}{\partial \theta}\frac{d\theta}{dt} - \omega_e \lambda_d\left(i_d, i_q, \theta\right) \end{aligned} \tag{9}$$

The self and cross-coupling dynamic inductances are defined as:

$$L_{dd}^{dyn} = \frac{\partial \lambda_d\left(i_d, i_q, \theta\right)}{\partial i_d} \tag{10}$$

$$L_{dq}^{dyn} = \frac{\partial \lambda_d\left(i_d, i_q, \theta\right)}{\partial i_q} \tag{11}$$

$$L_{qd}^{dyn} = \frac{\partial \lambda_q\left(i_d, i_q, \theta\right)}{\partial i_d} \tag{12}$$

$$L_{qq}^{dyn} = \frac{\partial \lambda_q\left(i_d, i_q, \theta\right)}{\partial i_q} \tag{13}$$

Finally, the total torque expression derived through co-energy is [27]:

$$T_e = \frac{3}{2}\frac{p}{2}\left(\lambda_d\left(i_d,i_q,\theta\right)i_q - \lambda_q\left(i_d,i_q,\theta\right)i_d\right) + \frac{3}{2}\left(\frac{\partial\lambda_q\left(i_d,i_q,\theta\right)}{\partial\theta}i_q + \frac{\partial\lambda_d\left(i_d,i_q,\theta\right)}{\partial\theta}i_d\right) - \frac{\partial W\left(i_a,i_b,i_c\theta\right)}{\partial\theta} \quad (14)$$

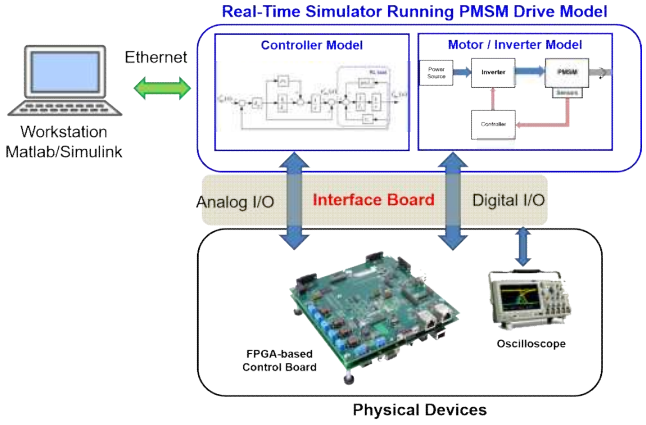

Fig. 11. Flow diagram of equations (1)-(14)

The flow diagram of Equations (1)-(14) is provided in Fig. 11. It is particularly useful to use these analytical expressions to predict instantaneous current ripple and torque ripple accounting for the effects of temperature variation, saturation, cross coupling, and spatial harmonics. Temperature variation must also be considered to ensure that machine parameters are as accurate as possible (Fig. 11).

C. Analytical Modeling Techniques

HIL simulation that uses analytical models of induction motors [29, 30] and PMSM [31] has received a great deal of attention from researchers seeking improvements computational efficiency. An IM model based on a magnetic equivalent circuit (MEC) that accounted for magnetic saturation was previously developed by [29], while [30] developed a real-time IM model based on nonlinear permeance network (PN). An analytical PMSM model based on linear field equations (LFE) that accounted for spatial harmonics was proposed in [31].

While these proposed and published models do have certain disadvantages, including a lack of generality and reliance on simplifying assumptions, their low computational cost and provision of useful insights into the physicality of electric machines means that each may be appropriately relied on at an early development stage.

D. Machine Parameter Identification

HIL simulation performance improves along with the accuracy of machine parameter determination. Previously published parameter identification methods either adopt an online and offline strategy [32]. Online parameter identification refers to real-time parameter estimation that rely on experimental setup and measurement devices, whereas the offline parameter estimation relies on experimental methods in conjunction with FE/analytical calculations. In this subsection, we summarized information relevant to offline methods.

1) Experimental Method

The experimental methods developed in [33-37] require a speed-controlled prime mover with two motors connected back-to-back, as shown in Fig. 12. The shaft rotation allows parameter extractions for no-load and loaded conditions. The excitation signals are generated by either sine wave generators [38, 39] or PWM drives [40-42]. The offline method in [43] presents the measured *dq* flux linkages of a tested machine to highlight magnetic saturation and cross-couplings (Fig.13). Other experimental methods include dc standstill tests [44, 45] and self-commissioning [46, 47]. Further details related to parameter identification may be found in [32].

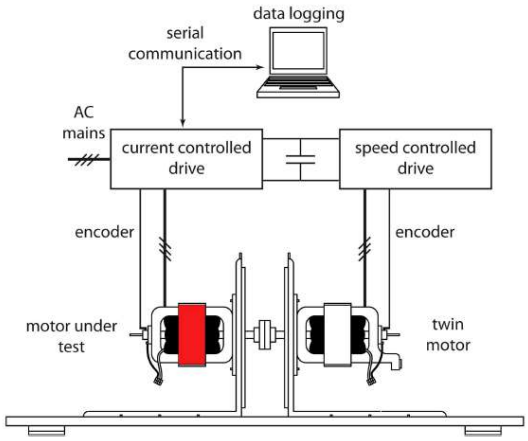

Fig. 12. Experimental setup [42]

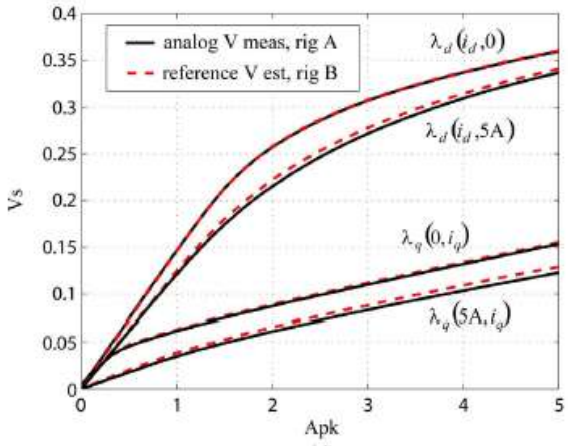

Fig. 13. Measured *dq* flux linkages [42]

2) FEA and Analytical Methods

Where experimental data is not readily available, then machine parameters should be extracted using FE simulation or analytical equations. The works presented in [48-52] illustrate various parameter identification methods. A dynamic *dq* equations-based method that uses FE-calculated parameters was proposed in [50]. The authors of [51] compared experimental results with *dq* synchronous reactance of PMSMs as previously determined through analytical and FE methods. A similar hybrid method that combines analytical expressions and FE calculations to obtain the *dq* inductances of PMSM, including the saturation and cross-coupling effects, was presented in [52]. It is also clear from [53, 54] that the computational efforts associated with FE analysis can be

significantly reduced even as accuracy is improved by exploiting the slot-pitch symmetry and the periodicity of the electromagnetic field.

FE and analytical models may be less accurate than those derived from experimental methods as a result of several factors, including as motor material properties (e.g., magnet properties, lamination steel properties), manufacturing tolerances (e.g., geometrical errors), and manufacturing effects (e.g., stamping, welding), as well as unaccounted-for end effects stemming from 2D analysis.

E. Machine Losses and Temperature Effect

dq equations are typically performed with simplifying assumptions in which the impacts of temperature variation and machine losses are disregarded, resulting in potential errors if the device under HIL simulation is sensitive to such factors.

Core losses have generally been neglected in the research, although we note that such can be taken accounted for by introducing a virtual damping winding [55]. Loss lookup tables can also be incorporated into a simulation through either an analytical method or through FE analysis. Care must be taken when simulating systems that will operate in a wide range of temperature as there may be significant thermal impacts on permanent magnets and copper windings; temperature variation affects magnet remanence, coercivity, copper resistivity, and the resulting stator flux linkages as well as developed torque. The machine parameters in Equations (1)-(14) can be calculated at different temperatures using FE analysis by assuming temperature-dependent material properties [57].

F. Machine Model under Fault Conditions

Electric drive systems are increasingly used in safety-critical systems like electric vehicles and aircrafts. HIL systems have become an integral part of the development and testing of these systems, which would otherwise have to go through destructive and expensive verification processes. However, emulating such applications poses a challenge, insofar as it necessitates the development of a model truly capable of simulating fault scenarios. To address this issue, a number of analytical and numerical methods have been proposed to date.

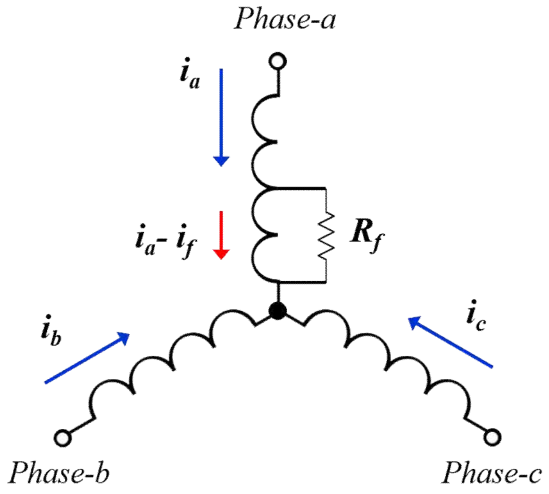

Fig. 14. Stator winding interturn short-circuit fault.

An *abc* phase variable model with constant inductances has been used to emulate the dynamics of a machine with interturn short-circuits in the stator winding [56]. A fault model of an inverter-fed PMSM drive has been developed to analyze interturn short-circuit and inverter switch open-circuit faults [57]. Since balanced three-phase conditions do not hold under these fault circumstances, the developed fault model is based on line-to-line voltage equations with phase variables. In [58], analytical expressions that include spatial harmonics and transient effect were developed for surface PMSMs with interturn short-circuits, though the effect of magnetic saturation was not considered. An FE-based phase variable model was proposed by [59] to analyze PMSM characteristics with interturn short-circuit faults. The machine parameters, including back-emf voltage and inductances, were predicted using FE-circuit coupled analysis. Interturn short-circuit fault models for PMSMs with both series and parallel winding connections were developed in [60]. These models were developed for positive and negative sequence *dq* synchronous reference frames.

Machine models based on FE-calculated flux linkage maps as a function of *dq* stator currents and rotor position are promising in terms of accuracy and calculation time [61, 62]. Such models are computationally efficient, and will be useful in the development of diagnostic algorithms and remedial strategies under interturn fault conditions, such as those shown in Fig.14, and which includes the nonlinear effects of saturation and spatial harmonics. According to equations in [62], the analytical *dq* model in the synchronous reference frame can be expressed as:

$$v_d = R_s i_d + \frac{d\lambda_d}{dt} - \omega_e \lambda_q - \frac{2}{3}\mu R_s \sin\left(\theta + \frac{2\pi}{3}\right) i_f \quad (15)$$

$$v_q = R_s i_q + \frac{d\lambda_q}{dt} + \omega_e \lambda_d - \frac{2}{3}\mu R_s \sin\left(\theta + \frac{2\pi}{3}\right) i_f \quad (16)$$

$$v_f = \mu R_s \left(i_d \sin\left(\theta + \frac{2\pi}{3}\right) + i_q \cos\left(\theta + \frac{2\pi}{3}\right) - i_f \right) + \frac{d\lambda_f}{dt} \quad (17)$$

Both the *dq* flux linkages and the flux linkage in the faulted turns, λ_f, are given by four-dimensional lookup tables.

V. CONCLUSION

In this paper we reviewed some newly developed advanced HILS implementation approaches applicable to the design and manufacture of electric machine drives. Our review encompassed two categories of HILS implementation, commercial real-time machines and practical modeling methods for electric machine drives. HILS systems that utilize commercial real-time machines and automatically generate code allow for speedier and more cost-effective development of electric machine drives than HILS that employ DSP or FPGA. As each real-time machine is different in terms of functions and affordability, users will have to think carefully about which machine is the most well-suited to their particular application. We also explored the accuracy with which control target systems can be modelled, and reviewed mathematical and analytical modeling techniques for PMSM drives, as well as

various machine parameter identification methods. Finally, we examined new insights into modeling techniques that account for operating conditions such as temperature and fault conditions. We anticipate that researchers will continue to push for more efficient, reliable, accurate, and practical HILS systems.

REFERENCES:

[1] I.R.Kendall and R. P. Jones, "An investigation into the use of hardwarein-the-loop simulation testing for automotive electronic control systems," *Control Eng. Pract.*, vol. 7, no. 11, pp. 1343–1356, Nov. 1999.

[2] T. N. Chang, B. Cheng, and P. Sriwilaijaroen, "Motion control firmware for high-speed robotic systems," *IEEE Trans. Ind. Electron.*, vol. 53, no.5, pp.1713-1722, Oct. 2006.

[3] L. Gauchia and J. Sanz, "A per-unit hardware-in-the-loop simulation of a fuel cell/battery hybrid energy system," *IEEE Trans. Ind. Electron.*, vol. 57, no. 4, pp. 1186–1194, Apr. 2010.

[4] L. Hui, M. Steurer, K. L. Shi, S. Woodruff, and Z. Da, "Development of a unified design, test, and research platform for wind energy systems based on hardware-in-the-loop real-time simulation," *IEEE Trans. Ind. Electron.*, vol. 53, no. 4, pp. 1144–1151, Jun. 2006.

[5] H. Sunan and T. Kok Kiong, "Hardware-in-the-loop simulation for the development of an experimental linear drive," *IEEE Trans. Ind. Electron.*, vol. 57, no. 4, pp. 1167–1174, Apr. 2010.

[6] W. Ren, M. Steurer, and T. L. Baldwin, "Improve the stability and the accuracy of power hardware-in-the-loop simulation by selecting appropriate interface algorithms," *IEEE Trans. Ind. Appl.*, vol. 44, no. 4, pp. 1286–1294, Jul./Aug. 2008.

[7] J. J. Rodríguez-Andina,M. J.Moure, andM. D. Valdés, "Features, design tools, and application domains of FPGAs," *IEEE Trans. Ind. Electron.*, vol. 54, no. 4, pp. 1810–1823, Aug. 2007.

[8] E. Monmasson, L. Idkhajine, and M. W. Naouar, "FPGA-based controllers," *IEEE Ind. Electron. Mag.*, vol. 5, no. 1, pp. 14–26, Mar. 2011.

[9] L. Gomes, E. Monmasson, M. Cirstea, and J. J. Rodríguez-Andina, "Industrial electronic control: FPGAs and embedded systems solutions," in *Proc. 39th Annu. Conf. IEEE Ind. Electron. Soc. (IECON'13)*, 2013, pp. 60–65.

[10] Dr.-Ing Joachim Bocker, M. Sun, Z. Cao, L Tong, H Zou and P Ranjan, "High Fidelity Hybrid Hardware-in-the-Loop Simulator with FPGA and Processor for AC Railway Traction", PCIM Nuremberg, Europe, pp.822-829, May 2012.

[11] Alberto Sanchez, Angel de Castro and Javier Garrido, "A comparison of simulation and Hardware-In-the Loop Alternatives for digital control of power converters," *IEEE Trans. on Ind. Informatics*, vol. 8, No.3, pp. 491-500, Aug. 2012.

[12] C.Choi and W.Lee, "Analysis and compensation of time delay effects in hardware in the loop simulation for automotive PMSM drive system", *IEEE Trans. on Ind. Electr,* vol. 59, No.9, pp. 3403-3410, Sept. 2012.

[13] https://www.speedgoat.com/products-services/real-time-target-machines

[14] https://www.dspace.com/en/pub/home/products/products.cfm#filterterms=term-325

[15] https://www.plexim.com/products/rt_box

[16] https://www.ni.com/en-us/shop/compactrio.html

[17] https://www.typhoon-hil.com/hil-hardware/

[18] https://www.rtds.com

[19] https://www.opal-rt.com/hardware-overview

[20] https://imperix.com/products/control/bbox

[21] M. Ojaghi and J. Faiz, "Extension to multiple coupled circuit modeling of induction machines to include variable degrees of saturation effects," *IEEE Trans. Magn.*, vol. 44, no. 11, pp.4053-4056, Nov. 2008.

[22] Z. Ling, L. Zhou, S. Guo, and Y. Zhang, "Equivalent circuit parameters calculation of induction motor by finite element analysis," *IEEE Trans. Magn.*, vol. 50, no. 2, pp. 833–836, Feb. 2014.

[23] O.A. Mohammed, Z. Liu, and S. Liu, "A novel sensorless control strategy of doubly fed induction motor and its examination with the physical modeling of machines," *IEEE Trans. Magn.*, vol. 41, no. 5, pp.1852-1855, May 2005.

[24] Y. Kano, K. Watanabe, T. Kosaka, and N. Matsui, "A novel approach for circuit-field-coupled time-stepping electromagnetic analysis of saturated interior PM motors," *IEEE Trans. Ind. Appl.*, vol. 45, no. 4, pp. 1325–1333, Jul./Aug. 2009.

[25] N. Bianchi and L. Alberti, "MMF harmonics effect on the embedded FE analytical computation of PM motors," *IEEE Trans. Ind. Appl.*, vol. 46, no. 2, pp. 812–820, Mar./Apr. 2010.

[26] X. Chen, J. Wang, B. Sen, P. Lazari, and T. Sun, "A high-fidelity and computationally efficient model for interior permanent-magnet machines considering the magnetic saturation, spatial harmonics, and iron loss effect," *IEEE Trans. Ind. Electron.*, vol. 62, no. 7, pp. 4044–4055, Jul. 2015.

[27] S. Li, D. Han and B. Sarlioglu, "Modeling of interior permanent magnet Machine Considering Saturation, Cross Coupling, Spatial Harmonics, and Temperature Effects," *IEEE Trans. on Trans. Elect.*, vol. 3, no. 3, pp. 682-693, Sept. 2017.

[28] L. Chang and T.M. Jahns, "Prediction and evaluation of PWM-induced current ripple in IPM machines incorporating slotting, saturation, and cross-coupling effects," *IEEE Trans. Ind. Appl.*, vol. 54, no. 6, pp. 6015–6026, Nov./Dec. 2018.

[29] B. Asghari and V. Dinavahi, "Experimental validation of a geometrical nonlinear permeance network based real-time induction machine model," *IEEE Trans. Ind. Electron.*, vol. 59, no. 11, pp. 4049–4062, Nov. 2012.

[30] N. R. Tavana and V. Dinavahi, "Real-time nonlinear magnetic equivalent circuit model of induction machine on FPGA for hardware-in-the-loop simulation," *IEEE Trans. Energy Convers.*, vol. 31, no. 2, pp. 520–530, Jun. 2016.

[31] N. R. Tavana and V. Dinavahi, "Real-time FPGA-based analytical space harmonic model of permanent magnet machines for hardware-in-the-loop simulation," *IEEE Trans. Magn.*, vol. 51, no. 8, pp. 1-9, Aug. 2015.

[32] S. A. Odhano, P. Pescetto, H. A. A. Awan, M. Hinkkanen, G. Pellegrino and R. Bojoi, "Parameter identification and self-commissioning in AC motor drives: a technology status review," *IEEE Trans. Power. Electron.*, vol. 34, no. 4, pp. 3603-3614, Apr. 2019.

[33] R. F. F. Koning, C. T. Chou, M. H. G. Verhaegen, J. Ben Klaassens, and J. R. Uittenbogaart, "A novel approach on parameter identification for inverter driven induction machines," *IEEE Trans. Control Syst. Technol.*, vol. 8, no. 6, pp. 873–882, Nov. 2000.

[34] D. M. Reed, H. F. Hofmann, and J. Sun, "Offline identification of induction machine parameters with core loss estimation using the stator current locus," *IEEE Trans. Energy Convers.*, vol. 31, no. 4, pp. 1549–1558, Dec. 2016.

[35] F. Alonge, F. M. Raimondi, G. Ferrante, and F. D'Ippolito, "Parameter identification of induction motor model using genetic algorithms," *IEE Proc.—Control Theory Appl.*, vol. 145, no. 6, pp. 587–593, Nov. 1998.

[36] R. Dutta and M. F. Rahman, "A comparative analysis of two test methods of measuring *d*- and *q*-axes inductances of interior permanent-magnet machine," *IEEE Trans. Magn.*, vol. 42, no. 11, pp. 3712-3718, Nov. 2006.

[37] A. Cavagnino, G. Pellegrino, S. Vaschetto and E. B. Agamloh, "Contribution to offline measurements of PMSM and SyRM inductances," *IEEE Trans. Ind. Appl.*, vol. 55, no. 1, pp. 407–416, Jan./Feb. 2019.

[38] B. Stumberger, B. Kreca, and B. Hribernik, "Determination of parameters of synchronous motor with permanent magnets from measurement of load conditions," *IEEE Trans. Energy Convers.*, vol. 14, no. 4, pp. 1413–1416, Dec. 1999.

[39] A. Tenconi, F. Profumo, M. Lazzari, and A. Cavagnino, "Axial flux interior PM synchronous motor: Parameters identification and steadystate performance measurements," *IEEE Trans. Ind. Appl.*, vol. 36, no. 6, pp. 1581–1588, Nov./Dec. 2000.

[40] K. Liu and Z. Q. Zhu, "Position offset-based parameter estimation for permanent magnet synchronous machines under variable speed control," *IEEE Trans. Power Electron.*, vol. 30, no. 6, pp. 3438–3446, Jun. 2015.

[41] K. Liu, J. Feng, S. Guo, L. Xiao, and Z.-Q. Zhu, "Identification of flux linkage map of permanent magnet synchronous machines under uncertain circuit resistance and inverter nonlinearity," *IEEE Trans. Ind. Inform.*, vol. 14, no. 2, pp. 556–568, Feb. 2018.

[42] K. M. Rahman and S. Hiti, "Identification of machine parameters of a synchronous motor," *IEEE Trans. Ind. Appl.*, vol. 41, no. 2, pp. 557–565, Mar./Apr. 2005.

[43] E. Armando, R. I. Bojoi, P. Guglielmi, G. Pellegrino and M. Pastorelli, "Experimental identification of the magnetic model of synchronous machines," *IEEE Trans. Ind. Appl.*, vol. 49, no. 5, pp. 2116–2125, Sept./Oct. 2013.

[44] L. Peretti and M. Zigliotto, "Automatic procedure for induction motor parameter estimation at standstill," *IET Electr. Power Appl.*, vol. 6, no. 4, pp. 214–224, Apr. 2012.

[45] K. Wang, W. Yao, B. Chen, G. Shen, K. Lee, and Z. Lu, "Magnetizing curve identification for induction motors at standstill without assumption of analytical curve functions," *IEEE Trans. Ind. Electron.*, vol. 62, no. 4, pp. 2144–2155, Apr. 2015.

[46] S. A. Odhano, P. Giangrande, R. I. Bojoi, and C. Gerada,"Self-commissioning of interior permanent-magnet synchronous motor drives with high-frequency current injection," *IEEE Trans. Ind. Appl.*, vol. 50, no. 5, pp. 3295–3303, Sept./Oct. 2014.

[47] S. A. Odhano, R. Bojoi, S. G. Ros¸u, and A. Tenconi, "Identification of the magnetic model of permanent-magnet synchronous machines using DC-biased low-frequency AC signal injection," *IEEE Trans. Ind. Appl.*, vol. 51, no. 4, pp. 3208–3215, Jul./Aug. 2015.

[48] G. Y. Sizov, D. M. Ionel, and N. A. O. Demerdash. "Modeling and parametric design of Permanent-magnet AC machines using computationally efficient finite-element analysis," *IEEE Trans. Ind. Electron.*, vol. 59, no. 6, pp. 2403–2413, Jun. 2012.

[49] K.Meessen, P. Thelin, J. Soulard, and E. Lomonova, "Inductance calculations of permanent-magnet synchronous machines including flux change and self- and cross-saturations," *IEEE Trans. Magn.*, vol. 44, no. 10, pp. 2324–2331, Oct. 2008.

[50] N. Bianchi and S. Bolognani, "Magnetic models of saturated interior permanent magnet motors based on finite element analysis," in *Conf. Rec. IEEE IAS Annu. Meeting*, Oct. 1998, vol. 1, pp. 27–34.

[51] K.Meessen, P. Thelin, J. Soulard, and E. Lomonova, "Inductance calculations of permanent-magnet synchronous machines including flux change and self- and cross-saturations," *IEEE Trans. Magn.*, vol. 44, no. 10, pp. 2324–2331, Oct. 2008.

[52] J. F. Gieras, E. Santini, and M. Wing, "Calculation of synchronous reactances of small permanent-magnet alternating-current motors: Comparison of analytical approach and finite element method with measurements," *IEEE Trans. Magn.*, vol. 34, no. 5, pp. 3712–3720, Sep. 1998.

[53] D.M. Ionel, M. Popescu, "Ultrafast Finite-Element Analysis of Brushless PM Machines Based on Space-Time Transformations," *IEEE Trans. Ind. Appl.*, vol. 47, no. 2, pp. 744-753, Mar./Apr. 2011.

[54] D.M. Ionel, M. Popescu, "Finite-element surrogate model for electric machines with revolving field—Applications to IPM motors," *IEEE Trans. Ind. Appl.*, vol. 46, no. 6, pp. 2424-2433, Nov./Dec. 2010.

[35] G. Luo, R. Zhang, Z. Chen, W. Tu, S. Zhang and R. Kennel, "A Novel Nonlinear Modeling Method for Permanent-Magnet Synchronous Motors," *IEEE Trans. Ind. Electron.*, vol. 63, no. 10, pp. 6490–6498, Oct. 2016.

[56] O.A. Mohammed, S. Liu, and Z. Liu, "FE-based physical phase variable model of PM synchronous machines under stator winding short circuit faults," *IET Science, Measurement & Technology*, vol. 1, no. 1, pp.12-16, Jan. 2007.

[57] K.-H. Kim, D.-U. Choi, B.-G. Gu, and I.-Su. Jung, "Fault model and performance evaluation of an inverter-fed permanent synchronous motor under winding shorted turn and inverter switch open," *IET Electr. Power Appl.*, vol. 4, no. 4, pp.214-225, Apr. 2010.

[58] I. Jeong, B.J. Hyon, and K. Nam, "Dynamic modeling and control for SPMSMs with internal turn short fault," *IEEE Trans. Power. Electron.*, vol. 28, no. 7, pp. 3495-3508, Jul. 2013.

[59] B. Vaseghi, N. Takorabet, and F. Meibody-Tabar, "Fault analysis and parameter identification of permanent-magnet motors by the finite-element method," *IEEE Trans. Magn.*, vol. 45, no. 9, pp.3290-3295, Sept. 2009.

[60] B. Gu, J. Choi, and I. Jung, "Development and analysis of interturn short fault model of PMSMs with series and parallel winding connections," *IEEE Trans. Power. Electron.*, vol. 29, no. 4, pp. 2016-2026, Apr. 2014.

[61] B. Sen, J. Wang, and P. Lazari, "A high fidelity, computationally efficient transient model of interior permanent magnet machine with stator turn fault," *IEEE Trans. Ind. Electron.*, vol. 63, no. 2, pp. 773–783, Feb. 2016.

[62] F. Alvarez-Gonzalez, A. Griffo, B. Sen and J. Wang, "Real-Time Hardware-in-the-Loop Simulation of Permanent-Magnet Synchronous Motor Drives Under Stator Faults," *IEEE Trans. Ind. Electron.*, vol. 64, no. 9, pp. 6960–6969, Sept. 2017.

Jae Suk Lee (S'07-M'14) received B.S. degrees from Inha University, Incheon, and Illinois Institute of Technology, Chicago, IL, USA, both in 2006, and the M.S. and Ph.D. degrees in electrical and computer engineering from the University of Wisconsin–Madison, Madison, WI, USA, in 2009 and 2013, respectively. Since 2014, he has been an Electrical Engineer with GE Global Research, Niskayuna, NY, USA. From 2015 to 2017, he was an Assistant Professor at Kyungnam University, Changwon, South Korea. He joined Jeonbuk National University, Jeonju, South Korea, in 2017, where he is currently an Associate Professor. His research interests are design and implementation of discrete-time control algorithms and observers for electric motor drives.

Gilsu Choi (S'07–M'16) received the B.S. degrees in electrical engineering from Inha University, Incheon, South Korea, and from the Illinois Institute of Technology, Chicago, IL, USA, both in 2008, and the M.S. and Ph.D. degrees in electrical engineering from the University of Wisconsin–Madison, Madison, WI, USA, in 2012 and 2016, respectively. In 2020, he joined the Department of Electrical Engineering, Inha University, Incheon, South Korea as an Assistant Professor. Prior to joining Inha University, he worked at General Motors Global Electrification Division, Pontiac, MI, USA, for 4 years. His research interests include design and control of high-performance electric machines and drives for electrified propulsion systems.

Dr. Choi was the recipient of second prize best paper awards from the IEEE Industry Applications Society Transportation Electrification Committee in 2017. He is an Associate Editor of the IEEE TRANSACTIONS ON INDUSTRY APPLICATIONS.